

et al., 2008; Thornton, Rousseau, & McGuckin, 2008). Initially, *N*-acetylgalactosaminyl peptidyltransferase transfers GalNAc to a serine or threonine when a nascent MUC polypeptide chain traverses the Golgi. The resulting *O*-glycan is then elongated in a stepwise manner by the addition of monosaccharides and monosaccharide derivative building blocks including galactose, GlcNAc, mannose and fucose, or by sialic acid (Brockhausen, Dowler, & Paulsen, 2009).

The stepwise building of mucin glycans with Gal and GlcNAc by glycosyltransferases leads to one of four core structures. Further to the addition of these sugars, these carbohydrate chains may also be substituted with *N*-acetylneuraminic acid and/or sulphate residues (Davril et al., 1999). Another important modification of core glycan chains, especially relevant to disease, is the formation of Lewis antigen structures, which are trisaccharide and tetrasaccharide capping groups and these may also be further sulphated and sialylated (Degroote, Ducourouble, Roussel, & Lamblin, 1999) (Fig. 1). *N*-acetylneuraminic acid and sulphate residues infer negative charges to mucins, affecting their polarity and acidity, whereas fucosylation increases mucin hydrophobicity. These modifications alter the physical properties of mucins and influence mucus rheology.

Alterations in mucin expression, secretion, glycosylation and Lewis antigen structures are characteristics of many respiratory diseases, including cystic fibrosis (CF) and chronic bronchitis (CB) (Davril et al., 1999; Degroote et al., 2003; Kirkham et al., 2008). Such changes are known to be influenced by inflammatory mediators, including cytokines and bacterial cell wall components. This response forms an important protective mechanism for inhibiting adhesion of potential pathogens and removal of irritants in the respiratory tract. It has been demonstrated that bronchial mucosa exposed to TNF α results in increased sialyltransferase activity and expression (Delmotte et al., 2002). This enzyme is specifically involved in Le^x synthesis, an epitope with high affinity to bind bacteria (Scharfman et al., 2001). Davril et al. have also shown that infected CF and CB patients have a greater concentration of sialic acid and sulphate residues on mucins compared to uninfected patients, correlated to an increase in expression of the sialyl-Le^x epitope (Davril et al., 1999). Fucose, a key structural component of the Le^x epitope, was also found to be increased by exposure to the endotoxin lipopolysaccharide (LPS), an inflammatory response mediator found in the outer membrane of gram-negative bacteria (Schroers, van der Marel, Neuhaus, & Steinhagen, 2009).

Secretion of mucins with altered terminal carbohydrate moieties alter the rheological and viscoelastic properties of mucus as addition of charged residues will influence mucin aggregation. In addition, fucose residues contained in Lewis antigen configurations will alter mucin solubility, affecting mucociliary clearance. In respiratory diseases the type of observed glycosylation change may vary with the progression status of the disease. Airway mucins in CB patients have been found to be less acidic (Davies et al., 1996; Kirkham et al., 2008), however, mucins are found to be more sialylated and sulphated in CB patients with severe infection and during disease exacerbation with increased levels of sialyl-Lewis x and sulfo-Lewis x structures (Davril et al., 1999; Lamblin et al., 2001; Loguidice et al., 1994) (Fig. 1). Several *O*-glycans from respiratory mucus from CF and CB patients have been characterised (Hounsell, 1994; Klein, Carnoy, Loguidice, Lamblin, & Roussel, 1992; Lamblin et al., 2001; Loguidice et al., 1994) and it appears that sialyl Le^x is more prevalent on glycoproteins in CF sputum, suggesting that increased expression of this epitope correlates with disease (Davril et al., 1999). Interestingly, sialyl Le^x and sLe^x determinants are known to interact with bacteria and viruses (Degroote et al., 1999; Scharfman et al., 2000) and these antigens are proposed as potential vaccines (Kufe, 2009) and antibody targets for chemotherapeutics (Boghaert et al., 2004).

Fourier transform infrared spectroscopy (FTIR) is a rapid, cost-effective and practical method for determining molecular structural change (Barth, 2007) and has shown potential in the analysis of glycoproteins and their component sugars (Khajehpour, Dashnau, & Vanderkooi, 2006). The key data derived from IR spectra is the band peak position due to molecular vibrations. Amide bonds have well defined absorption peaks and characteristic IR absorption patterns of sugars have been identified in the region of 950–1200 cm⁻¹ (Khajehpour et al., 2006). Furthermore, the applicability of FTIR for use as a diagnostic tool, based on distinct spectral changes observed in mucus, has already been described previously for respiratory disease including lung cancer (Lewis et al., 2010) and COPD (Whiteman, Yang, Jones, & Spiteri, 2008). In most studies that provide IR data from patient tissue, due to the heterogeneous mix of cellular molecules, the exact molecular cause of disease-specific IR spectral change remains unknown. Further work must be performed to attempt to correlate peaks observed in a disease spectrum with those produced for single or mixtures of molecules. Given the dominance of mucins in respiratory disease and specific changes in glycosylation, the aim of this study was to characterise the IR spectra for a range of mucin sugars and modified Lewis antigens. We anticipate that glycosylation specific IR patterns presented will assist in future studies to characterise disease specific structural changes in glycoproteins using IR technologies providing the potential for diagnostic technology development, disease progression monitoring and assessment of response to treatment.

2. Materials and methods

2.1. Fourier transform infrared spectroscopy

IR spectra were obtained with a Bruker Alpha Fourier Transform IR (FTIR) instrument equipped with a platinum ATR single reflection diamond sampling module (Bruker Optics). Samples were spotted directly onto the sampling module and left to air-dry at room temperature prior to spectral acquisition. Data points were collected as an average of 24 scans per sample between the wavenumber range of 450–4000 cm⁻¹ at a resolution of 4 cm⁻¹, controlled by Optics User Software (OPUS) version 6.5 (Bruker Optics). The process was repeated until six replicates were generated per sample. The resulting spectra were background corrected and smoothed using a nine-point Savitzky-Golay algorithm. Peak positions were determined using OPUS version 6.5 (Bruker Optics).

2.2. Monosaccharide and Lewis antigen FTIR analysis

IR spectra were generated for fucose, galactose, mannose, *N*-acetylglucosamine, *N*-acetylgalactosamine, sialic acid, Le^x, Le^y, Le^a and Le^b, sialyl-Le^x and sulfo-Le^x. Sugar films were obtained for analysis by preparing a solution of sugar in Milli-Q water at a concentration of 1 mg ml⁻¹. 3 μ l of sugar solution was placed on the FTIR sampling module for spectral acquisition. Lewis antigen spectra were generated at a concentration of 5 mg ml⁻¹ following identical methodology.

2.3. Sputum FTIR analysis

Spontaneous sputum was collected from a patient with COPD who was an ex-smoker with no symptoms for any other respiratory disease and not experiencing an exacerbation at the time of sputum collection. Therefore, the patient was considered representative of stable COPD with baseline characteristics and no bacterial or viral infection. Informed consent to provide a sputum sample was obtained as part of the Medlung observational study (loco-regional ethical committee approval 05/WMW01/75, study trial UKCRN ID

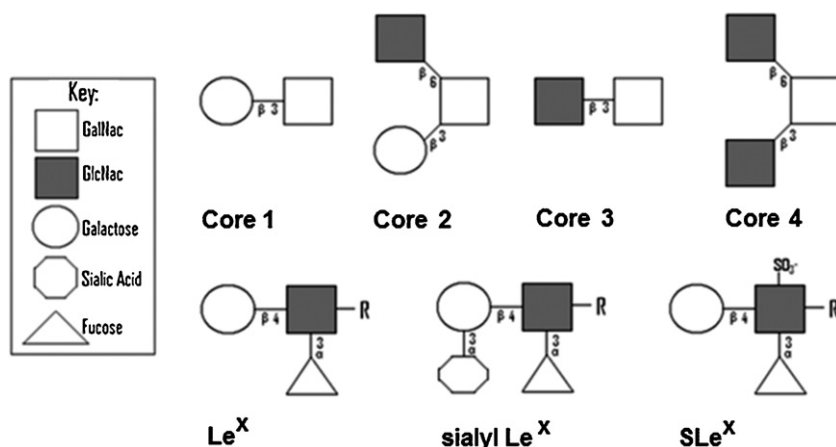


Fig. 1. Schematic representation of glycan oligosaccharide core structures 1–4, the Lewis x antigen and Lewis x derivatives. Le^x = Lewis x, sLe^x = sulfo-Lewis x and sialyl-Le^x = sialylated Lewis x.

4682). 3 μ l of raw sputum was placed onto the FTIR sampling module for spectral acquisition. IR absorbance peak positions within the COPD spectrum were compared to those within representative spectra of COPD and normal sputa published by others (Whiteman et al., 2008).

3. Results

3.1. IR spectra of monosaccharides found in mucin glycans

Infrared absorption spectra were generated for the monosaccharide building blocks found in mucin glycan cores. All spectra were deemed highly reproducible through repetition of the procedure using repeated samples.

Firstly, IR spectra were generated for mannose, fucose and galactose monosaccharides to establish the absorbance peak positions and intensities of each carbohydrate structure (Fig. 2). Spectra are reported within the range of 900–1280 cm^{-1} as it is within this region that the maximum IR absorbance due to the presence of carbohydrates is noted to occur (Khajehpour et al., 2006). Within this region, the following unique peaks associated with each monosaccharide were observed: mannose at 956 cm^{-1} , 971 cm^{-1} , 1020 cm^{-1} , 1047 cm^{-1} , 1167 cm^{-1} , 1251 cm^{-1} ; fucose peaks at 963 cm^{-1} , 996 cm^{-1} , 1027 cm^{-1} ,

1057 cm^{-1} , 1095 cm^{-1} , 1131 cm^{-1} , 1164 cm^{-1} , 1216 cm^{-1} and galactose peaks at 1037 cm^{-1} , 1068 cm^{-1} , 1143 cm^{-1} , 1249 cm^{-1} .

We then generated IR spectra for sugar derivatives, including *N*-acetylglucosamine, *N*-acetylgalactosamine and sialic acid. These monosaccharides also present a unique IR absorption pattern in the carbohydrate region of the spectrum, with distinguishable major peaks (Fig. 3): sialic acid absorption peaks occur at 1024 cm^{-1} , 1068 cm^{-1} , 1125 cm^{-1} , 1142 cm^{-1} , 1210 cm^{-1} , 1238 cm^{-1} ; GalNAc peaks at 976 cm^{-1} , 1038 cm^{-1} , 1076 cm^{-1} , 1095 cm^{-1} , 1115 cm^{-1} , 1153 cm^{-1} , 1219 cm^{-1} and GlcNAc peaks at 961 cm^{-1} , 1025 cm^{-1} , 1079 cm^{-1} , 1103 cm^{-1} .

3.2. IR spectra of Lewis antigens and modified derivatives

In comparing the absorption spectra for the Lewis antigens (Fig. 4) within the carbohydrate associated region of the spectra it can be seen that peak position and associated absorbance levels are extremely similar, which is to be expected based on their monosaccharide compositions. Major shared peaks occur at 968 cm^{-1} , 1033 cm^{-1} , and 1074 cm^{-1} . However, low-frequency vibrations attributed to glycosidic linkages also contribute to the spectra. The Lewis b and y antigens both contain a second fucose residue in an α -2 glycosidic linkage to galactose which may account for a wavenumber shift at peaks around 1164 cm^{-1} . Furthermore,

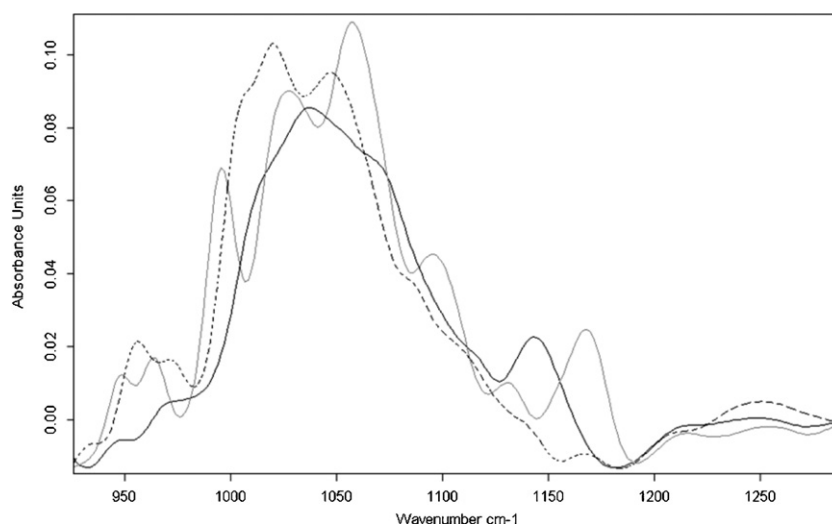


Fig. 2. IR spectrum of monosaccharides. Baseline corrected, smoothed, vector normalised spectrum of mannose (black dashed), fucose (grey) and galactose (solid black).

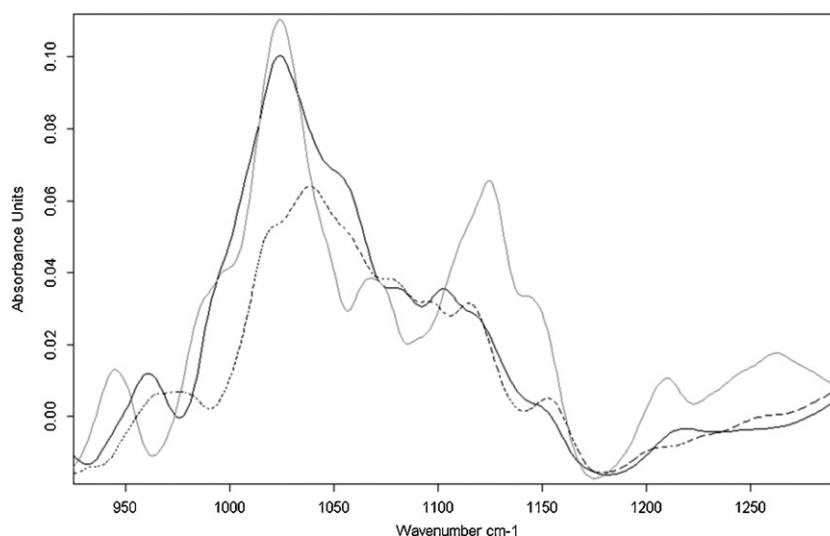


Fig. 3. IR spectrum of sugar derivatives and sialic acid. Baseline corrected, smoothed, vector normalised spectrum of sialic acid (solid grey), GalNAc (solid black) and GlcNAc (black dashed).

fucose residues linked to GlcNAc via an α -3 linkage could account for the unresolved peak at around 1020 cm^{-1} , prominent in the Lewis x (Le^x) spectrum, present in the Lewis y spectrum but absent in both Lewis a and b.

3.3. IR spectra of Le^x , sulfo- Le^x and sialyl- Le^x

The unmodified Le^x spectrum was compared to sialylated and sulphated versions, sialyl- Le^x and sulfo- Le^x (Fig. 5). The most clear difference between the three spectra is the sulphate associated ν_3 band of s Le^x appearing as a broad peak centred at around 1240 cm^{-1} and a narrower ν_1 band at 990 cm^{-1} (Nakamoto, 1986). This characteristic sulphate absorption thus allows the sulphated Lewis x derivative to be distinguished from the non-sulphated antigen. Spectral variation also occurred between 1100 cm^{-1} and 1200 cm^{-1} . A unique peak at 1130 cm^{-1} is only associated with the sialyl- Le^x antigen allowing differentiation from unmodified Le^x . Both Le^x and sialyl- Le^x also shared a peak position at 1160 cm^{-1} although this absorption in the sialyl- Le^x spectrum is reduced. The contribution of the sialic acid moiety to the sialyl Le^x spectrum

was examined by comparing the IR absorption of Le^x , sialyl- Le^x and sialic acid (Fig. 6). A sialic acid peak at 1125 cm^{-1} , whereas not present in the Le^x spectrum, appears to cause a peak shift in absorbance to 1130 cm^{-1} in the sialyl- Le^x spectrum likely due to influence of the additional absorbance of sialic acid at 1142 cm^{-1} .

3.4. IR spectra of sputum compared to sulfo- Le^x and sialyl- Le^x

Absorption spectra for sulfo- Le^x and sialyl- Le^x were compared to a typical raw sputum spectrum in the fingerprint region of $900\text{--}1280\text{ cm}^{-1}$ from a COPD patient (Fig. 7) (Table 1). The raw sputum spectrum showed the same pattern of absorbance as representative IR spectra of COPD patients published previously when compared to normal controls (Whiteman et al., 2008). The first observation was that this alignment clearly shows that the IR spectrum for sputum is highly similar to the general pattern for Le^x derivatives. Two key observations were noted. Firstly, a peak at 1240 cm^{-1} exists in the sputum sample spectrum corresponding with the characteristic sulphation peak. Secondly, a peak occurs at 1160 cm^{-1} with reduced absorbance in the sputum sample having

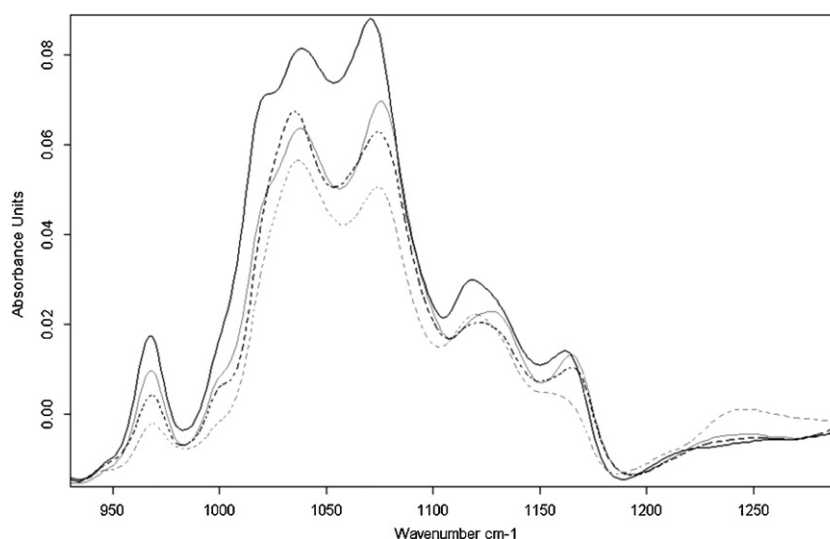


Fig. 4. IR spectrum of Lewis antigens. Baseline corrected, smoothed, vector normalised spectrum of Lewis a (grey dashed), Lewis b (black dashed), Lewis x (solid black) and Lewis y (solid grey).

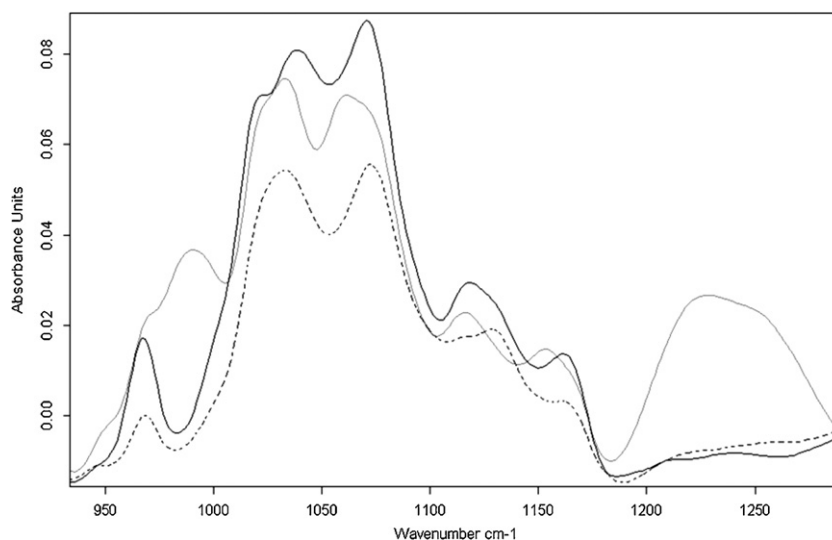


Fig. 5. IR spectrum of Lewis x and derivatives. Baseline corrected, smoothed, vector normalised spectrum of Lewis x (solid black), sialyl-Le^x (black dashed) and sulfo-Le^x (solid grey).

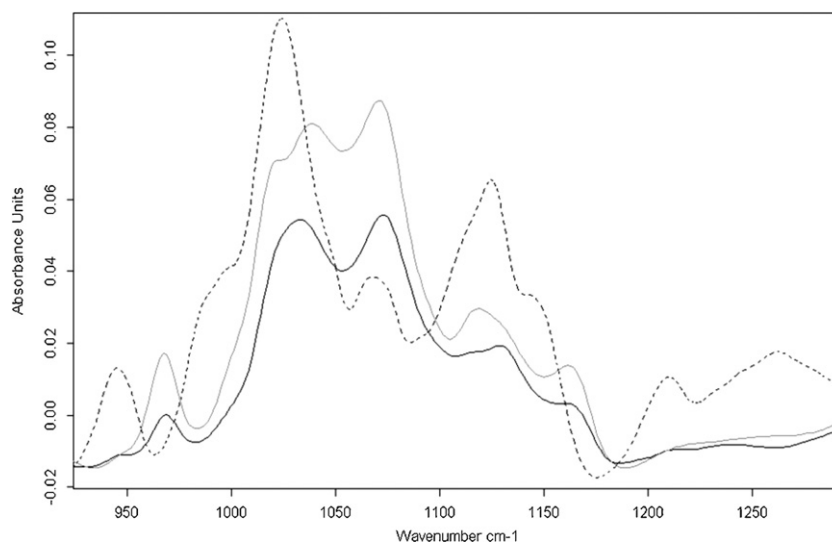


Fig. 6. Lewis x, sialyl-Le^x and sialic acid. Baseline corrected, smoothed, vector normalised spectrum of Lewis x (grey), sialic acid (black dashed) and sialyl-Le^x (solid black).

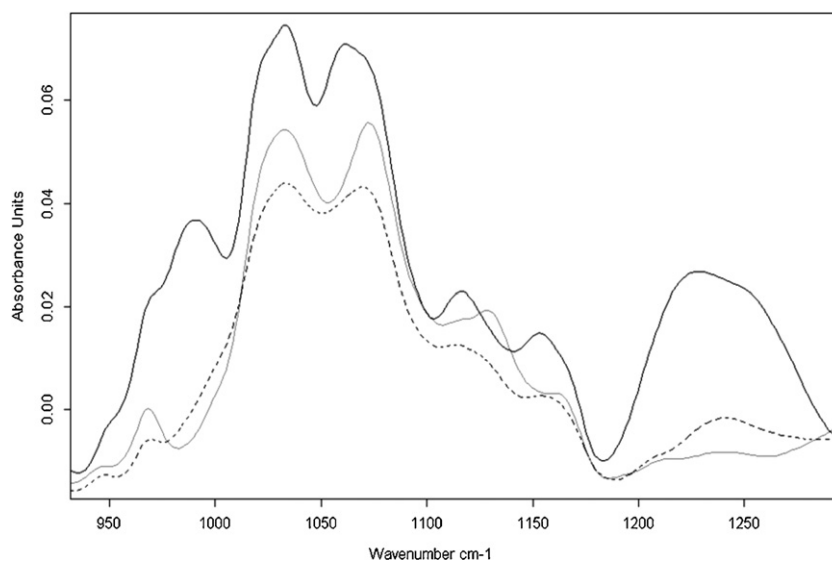


Fig. 7. COPD sputum, sialyl-Le^x and sulfo-Le^x. Baseline corrected, smoothed, vector normalised spectrum of sulfo-Le^x (solid black), sialyl-Le^x (solid grey) and raw COPD sputum (black dashed).

Table 1Key IR wavenumbers and proposed structural change in Lewis x, sialyl-Le^x and sulfo-Le^x and COPD sputum.

	Le ^x	Sialyl-Le ^x	Sulfo-Le ^x	Sputum	Proposed vibrational mode	Proposed primary source
IR Wavenumbers (cm ⁻¹)	968	968	968	969	ω (C—H)	Protein/sugar
			990		ν (S—O)	Sulphate
	1039	1033	1033	1033	ν/δ (C—O)	Sugar
	1073	1073	1068	1070	ν/δ (C—O)	Sugar
	1116		1116	1116	ν (S=O)	Sulphate
		1130			ν (C—O)	Sugar
			1153		ν (S—O)	Sulphate
	1161	1161			ν (C—N)	Sialic acid/GlcNAc
			1240	1240	ν (S=O)	Sulphate

Key: ν , stretch; δ , bend; ω , wag.

the same pattern observed for sialyl-Le^x. This strongly suggests the presence of these epitopes in COPD sputum. The alignment shows that potential structural changes to this antigen in disease tissue would be detectable by FTIR.

4. Discussion

The major aim of this study was to evaluate the ability of FTIR spectra to characterise the IR pattern of the Lewis x antigen, which is a major carbohydrate component of mucin glycoproteins. In our study we have emphasised the importance of disease related structural change of Le^x in mucus (and consequently sputum) linked with respiratory disease (Kirkham, Sheehan, Knight, Richardson, & Thornton, 2002) but we propose that FTIR could detect such changes in a wide variety of disease types. Although FTIR only provides information on vibrations of chemical groups, this study has shown that it is possible to differentiate carbohydrates based on their infrared absorption peaks. In the present work we have identified a number of discrete sugar and sulphate associated infrared absorption peaks that can be used to predict the presence of the major mucin linked carbohydrates and mucin modifications observed in the IR spectrum of sputum.

Analysis has shown that infrared spectroscopy is sugar specific and is able to discriminate between sugar moieties based on molecular bond vibrations (Khajehpour et al., 2006). Polysaccharide spectra are also molecule-specific and not only contain peaks relating to monosaccharide components but also peaks inferring information on glycosidic linkage, providing details of carbohydrate conformation. In our study we focused primarily on IR absorption bands between the 900 cm⁻¹ and 1280 cm⁻¹ wavenumber range. Absorbance peaks in tissue within this range predominantly arise from C—O and C—C stretching and C—O—H bending (Hounsell, 1994). Unique absorption patterns due to composite vibrations of the sugar ring, CH wagging and OH flexing vibrations also occur in this region resulting in the formation of sugar-specific peaks in the spectra. Furthermore, lower frequency bands in the region of 950–1150 cm⁻¹ have been associated with glycosidic linkage (Kacurakova & Mathlouthi, 1996). Previous studies investigating the general absorbance profiles of sugars have shown that C—O stretching and C—O—H bending modes are comparable over a range of concentrations, e.g. the galactose related peaks described in our study correspond to those previously reported (Kacurakova & Mathlouthi, 1996). Such examples validate the reproducibility and specificity of the technique for sugar identification in samples. In conjunction with previous data (Khajehpour et al., 2006), our spectral data also show that FTIR is able to differentiate between mono and oligosaccharides.

As alterations in band positions and intensities were representative of carbohydrate structural changes we further analysed derivatives of Lewis antigens, particularly Le^x, due to the predicted association of these structural changes with respiratory disease (Lamblin et al., 2001). Absorption maxima in the mid IR region for

the four different Lewis antigens were deemed similar. Focusing on Le^x we were able to demonstrate major peak differences correlated with the presence of sulphate and sialic acid moieties. The major stretching mode absorption characteristic of sulphate can be seen as a broad peak centred around 1240 cm⁻¹. This is in agreement with a previous study by Powell et al. who showed that a broad spectral band at this position was predictive of a sulphated oligosaccharide (Powell, Turula, Dehaseth, Vanhalbeek, & Meyer, 1994). The IR spectrum we observed for sialic acid also had the same peak positions shown by Khajehpour et al. (Khajehpour et al., 2006) despite some differences in experimental conditions and technology.

Mucins undergo differential expression in a large number of diseased tissues and a number of studies have focused studies on assessing their clinical relevance in various cancers (Rachagani, Torres, Moniaux, & Batra, 2009). There is also much evidence to show that mucins undergo altered glycosylation in many cancers and blood group antigens on mucin side chains show promise as markers of disease occurrence and progression (Rachagani et al., 2009). Le^x and the sialyl-Le^x are both overexpressed in breast tumour cells and are deemed good markers of metastatic potential (Apostolopoulos & McKenzie, 1994). Expression of sialyl-Le^x is also associated with poor survival rates in gastric cancer most likely due to an increased metastatic potential in tumour cells by sialyl-Lewis moieties through interaction with selectins (Fukuda, 1996; Kansas, 1996; Kim, Borsig, Han, Varki, & Varki, 1999).

There is now considerable evidence that glycosylation changes occur within mucins in a number of non-cancer diseases particularly within the respiratory tract. A study by Lo-Guidice et al. identified nine sulphated carbohydrate chains on mucins from patients with CB and sulphated glycoproteins have also been noted to occur on respiratory mucins in a number of diseased patients. Davril et al. showed that sialylation of bronchial mucins was found to be increased in patients suffering from CB (Davril et al., 1999). They, along with others (Loguidice et al., 1994; Vanhalbeek et al., 1994), also showed that overexpression of the sialyl-Le^x epitope and mucin hypersialylation occurs in respiratory disease including patients suffering with CB. Increasing levels of mucin associated sulfo-Le^x and sialyl-Le^x in CF and CB are also linked with infection (Davril et al., 1999).

Preliminary results are from our study are promising, however FTIR analysis of complex samples has limitations as the technique is not able to determine the molecular structure of compounds, merely which chemical groups are present in a particular sample. Some molecular vibrations associated with infrared absorption are also ambiguous and can be attributed to multiple chemical groups. For the analysis of carbohydrates, these limitations can be overcome to a large extent by comparing data to a reference library of monosaccharides. For the analysis of carbohydrates in complex molecular samples such as sputum we propose validation of findings through a larger study, with a control group, where the presence and concentrations of individual glycans and their

modifications in each sample are confirmed by a secondary technique such as immunohistochemistry.

In this study, we have focused on the detection of carbohydrate structural modification using FTIR for the potential application in medical diagnostics. Perhaps the key result of our findings though is the ability of FTIR to detect fine molecular structural change in carbohydrate polymers that are distributed throughout biology. There is much scope in building monosaccharide libraries for the application of FTIR to study modifications to complex carbohydrate polymer structure in other research domains including analytical chemistry, chemical synthesis, isolation of natural products, food and brewing, biorefining and drug synthesis.

5. Conclusions

In our study, we have demonstrated that characteristic IR peaks of both sulfo-Le^x and sialyl-Le^x were also observed in preliminary analysis of sputum from a patient suffering with COPD. Diseased sputum shows changes in the carbohydrate associated region of FTIR spectra arising from changes in sputum composition, which contains mainly mucins (Rose & Voynow, 2006). The fact that FTIR is able to distinguish between unmodified, sulphated and sialylated Lewis antigens and show variable antigen-specific IR peaks in disease sputum potentially makes it a powerful tool in glycoprotein analysis in disease. We propose that detection of glycosylation structural changes involving Lewis antigens by FTIR has potential in the development of new technologies and methods for disease detection and monitoring. Importantly, this method could assist in identifying disease progression associated glycosylation changes that could guide the development of novel drug delivery systems, particularly in respiratory diseases. We are currently performing a larger study to evaluate FTIR for detecting specific glycosylation changes that determine disease progression in patients with CB and COPD. Similar studies should be performed to determine the sensitivity of FTIR to evaluate diagnosis and progression of other respiratory as well as non-respiratory diseases that could provide tissue through non-invasive means.

Funding

This work was funded by the National Institute for Social Care and Health Research (NISCHR), Welsh Government.

Acknowledgements

We would like to thank Miss Georgina Menzies for technical assistance.

References

Apostolopoulos, V., & Mckenzie, I. F. C. (1994). Cellular mucins – Targets for immunotherapy. *Critical Reviews in Immunology*, 14(3–4), 293–309.

Barth, A. (2007). Infrared spectroscopy of proteins. *Biochimica Et Biophysica Acta – Bioenergetics*, 1767(9), 1073–1101.

Boghaert, E. R., Sridharan, L., Armellino, D. C., Khandke, K. M., DiJoseph, J. F., Kunz, A., et al. (2004). Antibody-targeted chemotherapy with the calicheamicin conjugate hu3S193-N-acetyl gamma calicheamicin dimethyl hydrazide targets Lewisy and eliminates Lewisy-positive human carcinoma cells and xenografts. *Clinical Cancer Research*, 10(13), 4538–4549.

Brockhausen, I., Dowler, T., & Paulsen, H. (2009). Site directed processing: Role of amino acid sequences and glycosylation of acceptor glycopeptides in the assembly of extended mucin type O-glycan core 2. *Biochimica Et Biophysica Acta – General Subjects*, 1790(10), 1244–1257.

Carraway, K. L., Ramsauer, V. P., Haq, B., & Carraway, C. A. C. (2003). Cell signaling through membrane mucins. *Bioessays*, 25(1), 66–71.

Corfield, A., & Shukla, A. (2003). Mucins: Vital components of the mucosal defensive barrier. *Genomic/Proteomic Technology*, 3, 20–22.

Davies, J. R., Hovenberg, H. W., Linden, C. J., Howard, R., Richardson, P. S., Sheehan, J. K., et al. (1996). Mucins in airway secretions from healthy and chronic bronchitic subjects. *Biochemical Journal*, 313(Pt 2), 431–439.

Davril, M., Degroote, S., Humbert, P., Galabert, C., Dumur, V., Lafitte, J. J., et al. (1999). The sialylation of bronchial mucins secreted by patients suffering from cystic fibrosis or from chronic bronchitis is related to the severity of airway infection. *Glycobiology*, 9(3), 311–321.

Degroote, S., Ducourouble, M. P., Roussel, P., & Lamblin, G. (1999). Sequential biosynthesis of sulfated and/or sialylated Lewis x determinants by transferases of the human bronchial mucosa. *Glycobiology*, 9(11), 1199–1211.

Degroote, S., Maes, E., Humbert, P., Delmotte, P., Lamblin, G., & Roussel, P. (2003). Sulfated oligosaccharides isolated from the respiratory mucins of a secretor patient suffering from chronic bronchitis. *Biochimie*, 85(3–4), 369–379.

Delmotte, P., Degroote, S., Lafitte, J. J., Lamblin, G., Perini, J. M., & Roussel, P. (2002). Tumor necrosis factor alpha increases the expression of glycosyltransferases and sulfotransferases responsible for the biosynthesis of sialylated and/or sulfated Lewis x epitopes in the human bronchial mucosa. *Journal of Biological Chemistry*, 277(1), 424–431.

Fukuda, M. (1996). Possible roles of tumor-associated carbohydrate antigens. *Cancer Research*, 56(10), 2237–2244.

Hakomori, S. (1985). Aberrant glycosylation in cancer cell membranes as focused on glycolipids: Overview and perspectives. *Cancer Research*, 45(6), 2405–2414.

Hakomori, S. (1996). Tumor malignancy defined by aberrant glycosylation and sphingoglycolipid metabolism. *Cancer Research*, 56(23), 5309–5318.

Hounsell, E. F. (1994). Physicochemical analyses of oligosaccharide determinants of glycoproteins. *Advances in Carbohydrate Chemistry and Biochemistry*, 50(50), 311–350.

Kacurakova, M., & Mathlouthi, M. (1996). FTIR and laser-Raman spectra of oligosaccharides in water: Characterization of the glycosidic bond. *Carbohydrate Research*, 284(2), 145–157.

Kansas, G. S. (1996). Selectins and their ligands: Current concepts and controversies. *Blood*, 88(9), 3259–3287.

Khajepour, M., Dashnau, J. L., & Vanderkooi, J. M. (2006). Infrared spectroscopy used to evaluate glycosylation of proteins. *Analytical Biochemistry*, 348(1), 40–48.

Kim, Y. J., Borsig, L., Han, H. L., Varki, N. M., & Varki, A. (1999). Distinct selectin ligands on colon carcinoma mucins can mediate pathological interactions among platelets, leukocytes, and endothelium. *American Journal of Pathology*, 155(2), 461–472.

Kirkham, S., Kolsum, U., Rousseau, K., Singh, D., Vestbo, J., & Thornton, D. (2008). MUC5B is the major mucin in the gel phase of sputum in chronic obstructive pulmonary disease. *American Journal of Respiratory and Critical Care Medicine*, 178(10), 1033–1039.

Kirkham, S., Sheehan, J. K., Knight, D., Richardson, P. S., & Thornton, D. J. (2002). Heterogeneity of airways mucus: Variations in the amounts and glycoforms of the major oligomeric mucins MUC5AC and MUC5B. *Biochemical Journal*, 361, 537–546.

Klein, A., Carnoy, C., Loguidice, J. M., Lamblin, G., & Roussel, P. (1992). Separation of mucin oligosaccharide-alditols by high-performance liquid-chromatography on alkylamine-bonded silica columns – Effects of structural parameters. *Carbohydrate Research*, 236, 9–16.

Kufe, D. W. (2009). Mucins in cancer: Function, prognosis and therapy. *Nature Reviews Cancer*, 9(12), 874–885.

Lamblin, G., Degroote, S., Perini, J. M., Delmotte, P., Scharfman, A. E., Davril, M., et al. (2001). Human airway mucin glycosylation: A combinatorial of carbohydrate determinants which vary in cystic fibrosis. *Glycoconjugate Journal*, 18(9), 661–684.

Lewis, P. D., Lewis, K. E., Ghosal, R., Bayliss, S., Lloyd, A. J., Wills, J., et al. (2010). Evaluation of FTIR spectroscopy as a diagnostic tool for lung cancer using sputum. *BMC Cancer*, 10.

Loguidice, J. M., Wieruszkeski, J. M., Lemoine, J., Verbert, A., Roussel, P., & Lamblin, G. (1994). Sialylation and sulfation of the carbohydrate chains in respiratory mucins from a patient with cystic-fibrosis. *Journal of Biological Chemistry*, 269(29), 18794–18813.

Moniaux, N., Escande, F., Porchet, N., Aubert, J. P., & Batra, S. K. (2001). Structural organization and classification of the human mucin genes. *Frontiers in Bioscience*, 6, D1192–D1206.

Murray, R. K. (2009). *Harper's illustrated biochemistry*. New York/London: McGraw-Hill Medical/McGraw-Hill.

Nakamoto, K. (1986). *Infrared and Raman spectra of inorganic and coordination compounds*. New York: Wiley.

Powell, D. A., Turula, V., Dehaseth, J. A., Vanhalbeek, H., & Meyer, B. (1994). Sulfate detection in glycoprotein-derived oligosaccharides by artificial neural-network analysis Fourier-transform infrared-spectra. *Analytical Biochemistry*, 220(1), 20–27.

Rachagani, S., Torres, M. P., Moniaux, N., & Batra, S. K. (2009). Current status of mucins in the diagnosis and therapy of cancer. *Biofactors*, 35(6), 509–527.

Reis, C. A., Osorio, H., Silva, L., Gomes, C., & David, L. (2010). Alterations in glycosylation as biomarkers for cancer detection. *Journal of Clinical Pathology*, 63(4), 322–329.

Rose, M. C., & Voynow, J. A. (2006). Respiratory tract mucin genes and mucin glycoproteins in health and disease. *Physiological Reviews*, 86(1), 245–278.

Roussel, P., & Delmotte, P. (2004). The diversity of epithelial secreted mucins. *Current Organic Chemistry*, 8(5), 413–437.

Scharfman, A., Arora, S. K., Delmotte, P., Van Brussel, E., Mazurier, J., Ramphal, R., et al. (2001). Recognition of Lewis x derivatives present on mucins by flagellar components of *Pseudomonas aeruginosa*. *Infection and Immunity*, 69(9), 5243–5248.

Scharfman, A., Delmotte, P., Beau, J., Lamblin, G., Roussel, P., & Mazurier, J. (2000). Sialyl-Le(x) and sulfo-sialyl-Le(x) determinants are receptors for *P. aeruginosa*. *Glycoconjugate Journal*, 17(10), 735–740.

- Schroers, V., van der Marel, M., Neuhaus, H., & Steinhagen, D. (2009). Changes of intestinal mucus glycoproteins after peroral application of *Aeromonas hydrophila* to common carp (*Cyprinus carpio*). *Aquaculture*, 288(3–4), 184–189.
- Shental-Bechor, D., & Levy, Y. (2008). Effect of glycosylation on protein folding: A dose book at thermodynamic stabilization. *Proceedings of the National Academy of Sciences of the United States of America*, 105(24), 8256–8261.
- Thornton, D. J., Rousseau, K., & McGuckin, M. A. (2008). Structure and function of the polymeric mucins in airways mucus. *Annual Review of Physiology*, 70, 459–486.
- Vanhalbeek, H., Strang, A. M., Lhermitte, M., Rahmoune, H., Lamblin, G., & Roussel, P. (1994). Structures of monosialyl oligosaccharides isolated from the respiratory mucins of a non-secreter (O, Le(a+B-)) patient suffering from chronic-bronchitis – Characterization of a novel type of mucin carbohydrate core structure. *Glycobiology*, 4(2), 203–219.
- Whiteman, S. C., Yang, Y., Jones, J. M., & Spiteri, M. A. (2008). FTIR spectroscopic analysis of sputum: Preliminary findings on a potential novel diagnostic marker for COPD. *Therapeutic Advances in Respiratory Diseases*, 2(1), 23–31.